

Alma Mater Studiorum Università di Bologna
Archivio istituzionale della ricerca

A methodological approach to define the state of conservation of the stone materials used in the Cairo historical heritage (Egypt)

This is the final peer-reviewed author's accepted manuscript (postprint) of the following publication:

Published Version:

Rovella N., Aly N., Comite V., Ruffolo S. A., Ricca M., Fermo P., et al. (2020). A methodological approach to define the state of conservation of the stone materials used in the Cairo historical heritage (Egypt). *ARCHAEOLOGICAL AND ANTHROPOLOGICAL SCIENCES*, 12(8), 1-14 [10.1007/s12520-020-01126-x].

Availability:

This version is available at: <https://hdl.handle.net/11585/916971> since: 2023-02-22

Published:

DOI: <http://doi.org/10.1007/s12520-020-01126-x>

Terms of use:

Some rights reserved. The terms and conditions for the reuse of this version of the manuscript are specified in the publishing policy. For all terms of use and more information see the publisher's website.

This item was downloaded from IRIS Università di Bologna (<https://cris.unibo.it/>).
When citing, please refer to the published version.

(Article begins on next page)

This is the final peer-reviewed accepted manuscript of:

Rovella N.; Aly N.; Comite V.; Ruffolo S. A.; Ricca M.; Fermo P.; Alvarez de Buergo M.; La Russa M. F.: A methodological approach to define the state of conservation of the stone materials used in the Cairo historical heritage (Egypt)

ARCHAEOLOGICAL AND ANTHROPOLOGICAL SCIENCES VOL. 12 ISSN
1866-9557

DOI: 10.1007/s12520-020-01126-x

The final published version is available online at:

<https://dx.doi.org/10.1007/s12520-020-01126-x>

Terms of use:

Some rights reserved. The terms and conditions for the reuse of this version of the manuscript are specified in the publishing policy. For all terms of use and more information see the publisher's website.

This item was downloaded from IRIS Università di Bologna (<https://cris.unibo.it/>)

When citing, please refer to the published version.

A Methodological approach to define the state of conservation of the stone materials used in the Cairo historical heritage (Egypt)

Natalia Rovella¹, Nevin Aly², Valeria Comite³, Silvestro Antonio Ruffolo¹, Michela Ricca¹, Paola Fermo³, Monica Alvarez De Buergo⁴, Mauro Francesco La Russa^{*, 1}

¹ University of Calabria, Department of Biology, Ecology and Earth Sciences (DiBEST), 87036 Arcavacata di Rende, CS (Italy)

² Suez University, Department of Science and Engineering Mathematics, Faculty of Petroleum and Mining Engineering, 43512 Suez (Egypt)

³ University of Milan, Department of Chemistry, 20133 Milan (Italy)

⁴ Geosciences Institute IGEO (CSIC-UCM), Doctor Severo Ochoa 7, 28040 Madrid (Spain)

***corresponding author: mlarussa@unical.it**

Abstract

The use of stone materials in cultural heritage and architecture represents a practice that has its roots in ancient times. Stone Buildings, depending on the construction materials and their location in the urban context, are particularly vulnerable to weathering phenomena. These can be often accelerated by changes in environmental conditions linked mostly to the anthropic activities.

In this way, the present work is addressed on the minero-petrographic and geochemical characterization of samples taken from the built historical heritage in Cairo (Egypt), related to seven monumental areas. These sites have been chosen based on their historical importance, type of material, state of preservation and position in the Cairo context.

The construction materials used and their degradation products were studied comparing the results obtained by means of different analytical techniques such as polarized light Optical Microscopy (POM), Ion chromatography (IC), Fourier Transform Infrared Spectroscopy (FT-IR) along with the carbonaceous fraction, detected by using the Thermogravimetry (TG).

The results achieved demonstrated that black crusts and salt crystallization represent the most common and damaging degradation products affecting all the monumental sites. Moreover, the environmental pollution produced by industrial activities and vehicular traffic has been identified as main cause of these processes, followed by a marginal contribution of natural sources such as the sea spray. The data collected provide useful information to plan efficient conservation strategies in the future.

Keywords: black crusts; cultural heritage; conservation; degradation; Egypt; stone

Introduction

Conservation of built cultural heritage requires a good understanding of different decay phenomena of stones materials related to textural features and environmental conditions. Stone damage of monuments is an irreversible loss of cultural heritage, so that the scientific community enhanced the efforts towards their conservation all over the world (Fitzner et al. 2000). Natural processes, such as weathering and thermal stress, and anthropic processes, including pollution,

vandalism and unsuitable restoration can determine an increase of the degradation and alteration phenomena. In this scenario, sedimentary stones, mostly carbonate such as limestones, but also dolostones, constitute a highly representative group of materials in built heritage objects (Delgado Rodrigues and Ferreira Pinto 2019). The main degradation agents which easily may affect limestone can be summarized as soluble salts and black crusts. Salt crystallization is one of the most common decay processes affecting stone building materials. It generates pressure variation, depending on the size and type of rock pore. Their presence can be detected by a sugary white coating (efflorescence) on the surfaces and, once they crystallize, salt crystals within the rock (sub efflorescence) can promote further decay (Monte 1991; Pires et al. 2010). Black crusts represent one of the most common types of patina in areas protected against direct rainfall or water runoff in urban environments (Araoz 2008). The formation of black crusts occurs mainly on carbonate stones, whose interactions with an SO₂-enriched atmosphere lead to the transformation of calcite (CaCO₃) into gypsum (CaSO₄*2H₂O). For this reason, the conservation of the building stone heritage needs that a reliable analytical approach is applied, in order to define the relation between the intrinsic properties of the stones and the development of these processes. Ancient Egypt was regarded as the “state out of stone”, because the stone was the most important raw material used during the different periods of Pharaonic Egypt as well as Greco- Roman and Arab times (Klemm and Klemm 2001).

Nowadays, Cairo is a world heritage city. It contains possibly the finest collection of monuments in the Islamic world especially dated back to the medieval period. Indeed, Cairo's Islamic monuments are part of an uninterrupted tradition that spans over a thousand years of building activity. No other Islamic city can equal Cairo's spectacular heritage. It includes the greatest concentration of Islamic monuments in the world, and its mosques, mausoleums, religious schools, baths, and caravanserais, built by prominent patrons between the seventh and nineteenth centuries, are among the finest in existence (Khallaf, 2001).

Unfortunately, the rapid increase in environmental pollution of the last century seriously threatens the archaeological buildings in Cairo and made it necessary to conceive efficient conservation strategies to preserve this precious world heritage. In this regard, different studies underlined the importance to investigate firstly the building raw materials, mostly limestone, because they suffer from different deterioration and alteration phenomena such as black crust formation, chemical alterations, salts crystallization, disintegration, pitting, cracks, erosion, etc. (Davidson et al. 2000; Khallaf 2001; Fitzner 2002; Abdelmegeed and Hassan 2019).

The focus of this work is to perform a complete characterization of stone materials from different building heritage located in Historic Cairo. In particular, a diagnostic approach was applied in order to investigate the decay process involved in this case study and to define the effective state of conservation of the materials analysed. For this purpose, specimens from different built heritage, underwent a complete diagnostic protocol, precisely: petrographic analyses, ion chromatographic analyses, Infrared spectroscopic analyses and carbonaceous fraction analysis.

Materials and Methods

Historic Cairo covers an area of ~30 km squared, is located in the city centre and holds a large number of Islamic architecture (i.e. mosques, madrasas, hammam and fountains). It was founded in the 10th century by the Fatimid Caliphs (Anoniou 1999; Williams 2004) and became UNESCO Heritage in 1979.

Tertiary porous limestones coming from the local quarries of Mokattam and Helwan areas have been used for the construction of monuments in Cairo since Pharaonic times until today (Fitzner et al. 2002; Aly et al. 2015, 2018, 2020). Additionally, several buildings were reconstructed many times partially or completely over the centuries.

In this study, eighteen stone samples, including their degradation products, were taken from the main facades and walls of seven monumental sites such as Salah El-Din Citadel, the Tower of Bab Al Azab, the Manial Palace, and four

representative buildings of the Northern Mamluk cemetery, namely, the Sultan Faraj ibn Barquq Mosque, the Qaitbay Mosque, the Al Silahdar Mosque and the Qansuh Al-Ghuri Mausoleum (Fig. 1).

Table 1 reports the examined samples and a short description about e.g. typology, period of construction, position and height.

Suitable stainless steel tools, such as lancets and small chisels, were employed on a representative portion of the material, in relation to the different macroscopic degradation forms observed, mainly efflorescence, soiling and black crusts.

Table 1 List and information about the samples collected in Historic Cairo, constituted by degradation layer (DL) and stone substrate (LS: limestone substrate; QS: quartz arenite substrate). The historical information about the building epoch of the monuments was drawn from William (2004). The Coordinates in WGS84 system were acquired from Google Earth.

Site 1 - Salah El-Din Citadel (1176 – 1183 AD)					
Sample ID	Location	Description	Position	Height of sampling	WGS84 Coordinates
4	North-Western outer wall	DL + LS	Vertical Surface	250 cm	30.03043, 31.25791
6	North-Western outer wall	DL + LS	Vertical Surface	35 cm	
Site 2 - Tower of Bab Al Azab (1754 AD)					
Sample ID	Location	Description	Position	Height of sampling	WGS84 Coordinates
5	Western wall	DL + LS	Vertical Surface	25 cm	30.03106, 31.25816
7	Western wall	DL + LS	Vertical Surface	155 cm	
Site 3 – Manial Palace (1899-1929 AD)					
Sample ID	Location	Description	Position	Height of sampling	WGS84 Coordinates
8	Northern wall	DL + QS	Vertical Surface	45 cm	30.02744, 31.22897
9	Northern wall	DL + LS	Vertical Surface	20 cm	
10	Northern wall	DL + LS	Vertical Surface	30 cm	
- Northern Mamluk cemetery (13 th -15 th centuries AD)					
Site 4 Sultan Faraj ibn Barquq Mosque (1400-1411)					
Sample ID	Location	Description	Position	Height of sampling	WGS84 Coordinates
17	Main Facade	DL + LS	Vertical Surface	20 cm	30.04919, 31.27876
18	Main Facade	DL + LS	Vertical Surface	200 cm	
Site 5 - Qaitbay Mosque (1472-1474)					
Sample ID	Location	Description	Position	Height of sampling	WGS84 Coordinates
A	Main Facade	DL + LS	Vertical Surface	90 cm	30.04388, 31.27499
C	Main Facade	DL + LS	Vertical Surface	200 cm	
D	Main Facade	DL + LS	Vertical Surface	50 cm	
Site 6 - Al Silahdar Mosque (1344-1345)					
Sample ID	Location	Description	Position	Height of sampling	WGS84 Coordinates
F	Main Facade	DL + LS	Vertical Surface	100 cm	30.05249, 31.26187
G	Main Facade	DL + LS	Vertical Surface	50 cm	
Site 7 - Qansuh Al-Ghuri Mausoleum (1503-1505)					
Sample ID	Location	Description	Position	Height of sampling	WGS84 Coordinates
I	Main Facade	DL + LS	Vertical Surface	90 cm	30.04565, 31.26088

A complete characterization of stone materials and degradation products was obtained by the means of the following analytical techniques.

The petrographic analysis was performed in order to define: the main textural features of the substrate; the composition of the superficial layers; the state of conservation of the substrate. For this purpose, polarized optical microscopy (POM),

with a Zeiss Axiolab microscope (equipped with a digital camera to capture images), on polished thin sections and stratigraphic sections was carried out.

Ion chromatography (IC) was used to quantify the main anions and cations present on the superficial layers. Each sample underwent the following protocol: 2 mg of powder was placed in a test tube and treated with 10 mL of MilliQ water. The solutions were sonicated for 1 h, then centrifuged for 30 min and analysed by mean an HPLC (DIONEX DX 120). Cationic (Na^+ , K^+ , Ca^{2+} , Mg^{2+} and NH_4^+) and anionic (NO_3^- , SO_4^{2-} , Cl^-) species were determined for each sample.

Fourier Transform Infrared Spectroscopy (FT-IR) measurements were carried out to determine the mineralogical phases constituting the examined superficial layers. Analyses were performed through a Perkin Elmer Spectrum 100 spectrophotometer equipped with an ATR (attenuated total reflectance) accessory.

As regards the carbonaceous fraction, OC (organic carbon), EC (elemental carbon) and CC (carbonatic carbon) have been quantified. The TGA (Thermo-Gravimetric Analysis) instrument was used to quantify the carbon fraction. The analyses were carried out with a Mettler Toledo TGA/DSC 3 instrument that allows simultaneous TG and DSC analyses, in a range between 30-800°C, increasing the temperature with a speed of 20°C/minute in two different atmospheres, inert and oxidizing. Calculations were carried out for the determination of the carbonaceous fractions present in the crusts, through the study of standards following the procedure described in La Russa et al. (2017). In particular, the analytical protocol applied is a thermal method based of the different thermal behaviour of carbon fractions: while OC decomposes at a lower temperature (about 340 °C, atmosphere inert), EC (range at 400 and 600°C, atmosphere oxidizing), Ox (range at 400 and 600°C, atmospheres inert) and CC (range at 600 and 800°C, atmospheres inert and oxidizing) are stable up to high temperature. The analysed samples were previously powdered through the use of an agate mortar, carefully separating the black crust and the substrate through the use of a scalpel.

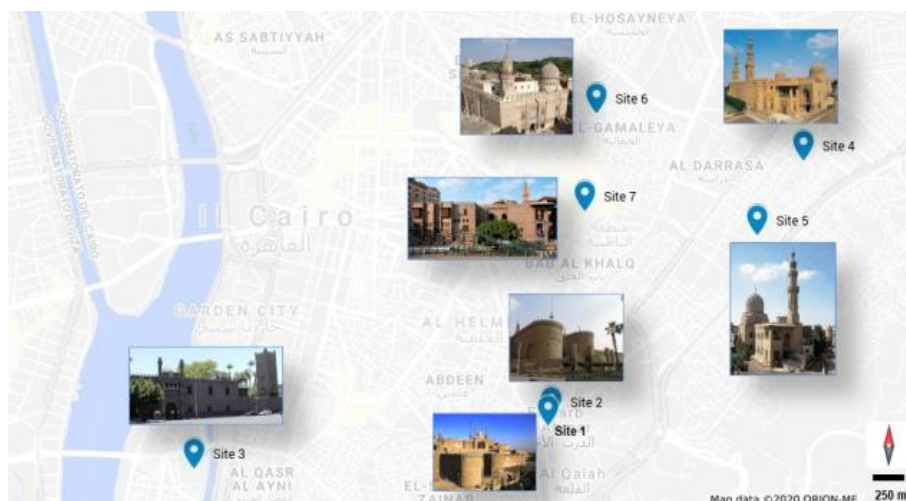


Fig. 1 Road map of Historic Cairo (Source Google maps modified). The blue icons and the photographs associated indicate the location of the sampled monuments. Site 1: Outer walls of Salah El-Din Citadel; Site 2: Tower of Bab Al Azab; Site 3: Manial Palace. Northern Mamluk cemetery area: Site 4: Sultan Faraj ibn Barquq Mosque (Image Credits: Discover Islamic Art - MWNF); Site 5: Qaitbay Mosque (Image Credits: Discover Islamic Art - MWNF); Site 6: Al Silahdar Mosque (Image Credits: Archive ARCE- American Research Centre in Egypt); Site 7: Qansuh Al-Ghuri Mausoleum (Image Credits: Archnet.org)

Results and discussions

Petrographic Analysis

Petrographic observations on thin sections revealed some remarkable variations regard to the adherence, thickness and morphology of the superficial layers on the substrate of the specimens and then on their state of conservation.

The main minero-petrographic features and the most representative microphotographs are reported respectively in Table 2 and Figure 2.

Samples, 4 and 6 were taken at different heights along the western external walls of the Salah El-Din Citadel (Site 1) and show different features both regard to the substrate and to the crust.

On the basis of textural features, Sample 4 can be classified such as biomicrite (Folk 1959) or mudstone (Dunham 1962) (Fig. 2a). The superficial layer, constituted by gypsum, shows a uniform thickness (about 50 μm) a good adherence, an irregular external morphology, brown colour and carbonaceous particles (Fig. 2a). These latter ones show a sub-spherical shape and averagely 30 μm in size. Regarding the state of conservation, the analysed sample seems to be poorly degraded. Sample 6 is an intrasparite (Folk 1959) or a packstone (Dunham 1962), where some quartz crystals and bioclasts are present. The superficial layer consists mainly of gypsum, is greyish in colour, with a homogeneous thickness (about 100 μm), irregular external morphology and contains sub-spherical carbonaceous particles. The degradation degree is suggested by microfractures along the contact between substrate and superficial layer, visible only in some portions.

Samples 5 and 7 come from the tower of Bab Al Azab (Site 2).

Sample 5 is a pelmicrite (Folk 1959) or a mudstone (Dunham 1962) with common quartz crystals. The superficial layer shows a variable thickness of around 200 μm , divided into two levels, both of about 100 μm (Fig. 2b). The outermost one is darker in colour, shows an irregular morphology, and a compact aspect. The innermost one is reddish in colour, with different microfractures (Fig. 2b). The substrate is in a good state of conservation.

Sample 7 is a biosparite according to Folk (1959) or a packstone (Dunham, 1962). The allochem component is mainly formed of quartz, opaque minerals, probably iron oxides, and also bioclasts such as Gastropods. The superficial layer is discontinuous; the thickness is variable, reaching 100 μm in some portions. The layer shows good adherence to the substrate, a rather regular external morphology and a colour ranging from brownish to black. It contains microcrystalline gypsum, quartz, iron oxides and sub-spherical carbonaceous particles 10-50 μm sized. The conservation degree of the substrate is fair with occasional phenomena of secondary dissolution of some bioclasts.

The samples 8, 9 and 10 were taken from the Manial Palace (Site 3).

Specimen 8 is a quartz arenite; on its surface it is clear the presence of a discontinuous deposit, brown in colour, with a variable thickness, the maximum being of 100 μm . The substrate shows a good state of conservation.

Sample 9 is a biosparite (Folk 1959) or a wackestone (Dunham 1962). The allochem fraction consists mainly of quartz, iron oxides and also bioclasts such as Macroforaminifera and Gastropods. The superficial layer is discontinuous, well adhered to the substrate, brownish in colour with a variable thickness, reaching 100 μm only in some points. The external morphology is irregular and the profile is jagged. Microcrystalline gypsum, quartz, iron oxides and subspherical carbonaceous particles were identified in the layer.

Sample 10 is a biomicrite (Folk 1959), with abundant bioclasts (> 10%) mainly represented by foraminifera; additionally, it is classifiable as packstone according to Dunham (1962). The alteration layer is not well adhered to the substrate, has a thickness ranging between 100 and 500 μm , dark in colour and jagged outer edge (Fig. 2c). Inside it, there are spherical carbonaceous particles and rare gypsum crystals.

Samples 17, 18 are related to the Sultan Faraj ibn Barquq Mosque (Site 4).

Sample 17 is a biosparite (Folk 1959) or wackestone (Dunham 1962). The alteration layer is present only in some areas with a thickness ranging from 10 to 50 μm , it is constituted by gypsum and common subspherical carbonaceous particles of about 10-20 μm in diameter.

Sample 18 is a biomicrite (Folk 1959) or a wackestone (Dunham 1962). The allochems are constituted by quartz, opaque minerals such as iron oxides, calcareous rock fragments and fossiliferous fragments (Fig. 2d). The superficial layer shows

a dendritic morphology, colour varying from greyish to brownish, it is separated by a fracture from the substrate (Fig. 2d). The thickness ranges from 200 μm to 400 μm . The layer includes microcrystalline gypsum, quartz, iron oxides and subspherical carbonaceous particles 30-50 μm sized.

Both substrates show a good state of conservation.

The samples A-C-D come from the Qaitbay Mosque (Site 5).

Sample A is an intramicrite (Folk 1959) or a wackestone (Dunham 1962). The superficial layer has a thickness of about 200 μm , is firmly attached to the substrate and shows a rather regular outer profile. Three levels are distinguishable: the outer layer has a dark brown colour and a thin thickness, it does not exceed 50 μm ; the intermediate layer has a greyish colour, with a variable thickness of around 100 μm and is particularly rich in carbonaceous particles; the innermost layer, at the interface with the substrate, is brownish and shows a variable thickness, from 20 to 50 μm .

Sample C is a biomicrite (Folk 1959) or a mudstone according to Dunham (1962). The allochems consist of iron oxides and fossils, in particular macroforaminifers such as Nummulites. The superficial layer is rather discontinuous, dark brown in colour, approximately 100 μm thick and well adherent to the substrate. Rare gypsum crystals iron oxides and carbonaceous particles were identified.

Sample D is a biomicrite (Folk 1959) with particularly abundant foraminifera, a wackestone according to Dunham's classification system (Dunham 1962). The superficial layer is brownish-gray, quite thin (about 50 μm and not more than 100 μm) and not regularly present on the substrate (Fig. 2e). Microcrystalline gypsum is the main component followed by few carbonaceous particles and iron oxides. Overall, the degree of conservation of the substrate in all the samples is rather good.

The samples F and G come from the Al Silahdar Mosque (Site 6).

Sample F is an intramicrite (Folk 1959) or mudstone (Dunham 1962), with quartz and plagioclase crystals inside (<10%). The superficial layer presents a variable thickness of about 100 μm , a good adherence to the substrate, and an irregular dendritic morphology. Additionally, it can be divided into two different levels: the outer one shows a dark brown colour, a thickness of approximately 70 μm and a good concentration of subspherical carbonaceous particles, 10-20 μm sized; the inner layer appears yellowish and thinner with a thickness of max 30 μm . The contact layer/substrate is rather continuous and sharp. The state of conservation is scarce because of different microfracture systems crossing the substrate. Sample G is a biomicrite (Folk 1959) or a wackestone (Dunham 1962). The allochemical components are constituted by quartz, plagioclase, iron oxides and bioclasts.

The superficial layer is present only partially on the substrate. The main composition is represented by microcrystalline gypsum, quartz, black and brown iron oxides, and subspherical carbonaceous particles 10-30 μm sized. The layer shows a brownish colour, the average thickness is about 100 μm .

Its adherence to the substrate is good in some points but discontinuous and irregular in others, where the layer pierces inside for max 50 μm by means of microfractures (Fig. 2f). For this reason, the state of conservation of the substrate is not considered good.

The sample I was taken from the Qansuh Al-Ghuri Mausoleum (Site 7). It is classified such as a biomicrite (Folk 1959) or a mudstone (Dunham 1962). The bioclasts are mainly foraminifera; the superficial layer is thin, with a variable thickness between 100 and 200 μm , it shows a blackish colour and a good adherence on the substrate (Fig. 2g). The main constituent is gypsum but there is also a low amount of quartz crystals. The state of conservation is fair since the layer can penetrate for about 50 μm in the substrate.

Overall, most substrates are constituted by limestone except for a quartz arenite (Sample 8). The classification criteria of Folk (1959) and Dunham (1962) suggest a certain compositional and textural heterogeneity coherently with the rocks

extracted in the local quarries. Mostly biomicrites were identified, followed by intramicrites and biosparites (Folk 1959), mudstone, wackestone, and finally packstone (Dunham 1962). The substrates inside, show a fair state of conservation with some cases of internal fracturing or secondary porosity, for example, relative to dissolution of the bioclasts. Conversely, all of them are affected by a superficial layer of alteration, generally discontinuous in samples 7, 8, 9, D, G, rather continuous in the others with an average thickness of 100 μm and reaching in some cases 400-500 μm (Samples 10 - 18). The contact layer/substrate is commonly linear and sharp, with a rare penetration of the layer inside by the means of some microfractures up to 50 μm (Samples F, G, I).

Table 2 summarises the main minero-petrographic features observed by OM about the substrate (according to Folk 1959 and Dunham 1962 classifications) and the superficial alteration layer. The state of conservation refers to the substrate as reported in the text and it is distinguished in poor, fair and good.

Legend: *: discontinuous and variable thickness. Abbreviations: Gy (gypsum); Qtz (quartz); Oxd (oxides); CP (Carbonaceous Particles). A (adherent to the substrate); N.A. (not well adherent to the substrate).

	Samples ID	Substrate	Alteration layer			State of Conservation
			Total Thickness	Morphology	Mineral Composition	
Site 1	4	biomicrite mudstone	50 μm	irregular A	Gy; CP	good
	6	intrasparite packstone	100 μm	irregular N.A.	Gy; CP	fair
Site 2	5	pelmicrite mudstone	200 μm	irregular N.A.	Gy; Qtz; Oxd; CP	good
	7	biosparite packstone	max 100 μm^*	regular A	Gy; Qtz; Oxd; CP	fair
Site 3	8	quartz arenite	max 100 μm^*	irregular A	Gy	good
	9	biosparite wackestone	max 100 μm^*	jagged A	Gy; Qtz; Oxd; CP	fair
	10	biomicrite packstone	100-500 μm	jagged N.A.	Gy; CP	fair
Site 4	17	biosparite wackestone	100-50 μm	irregular A	Gy; CP	good
	18	biomicrite wackestone	200-400 μm	dendritic N.A.	Gy; Qtz; Oxd; CP	good
Site 5	A	intramicrite wackestone	200 μm	regular A	Gy; CP	good
	C	biomicrite mudstone	100 μm^*	irregular A	Gy; Oxd; CP	good
	D	biomicrite wackestone	50- 100 μm^*	irregular N.A.	Gy; Oxd; CP	good
Site 6	F	intramicrite mudstone	100 μm	dendritic A	Gy; CP	poor
	G	biomicrite wackestone	max 100 μm^*	irregular N.A.	Gy; Qtz; Oxd; CP	fair
Site 7	I	biomicrite mudstone	100 - 200 μm	regular A	Gy; Qtz; CP	fair

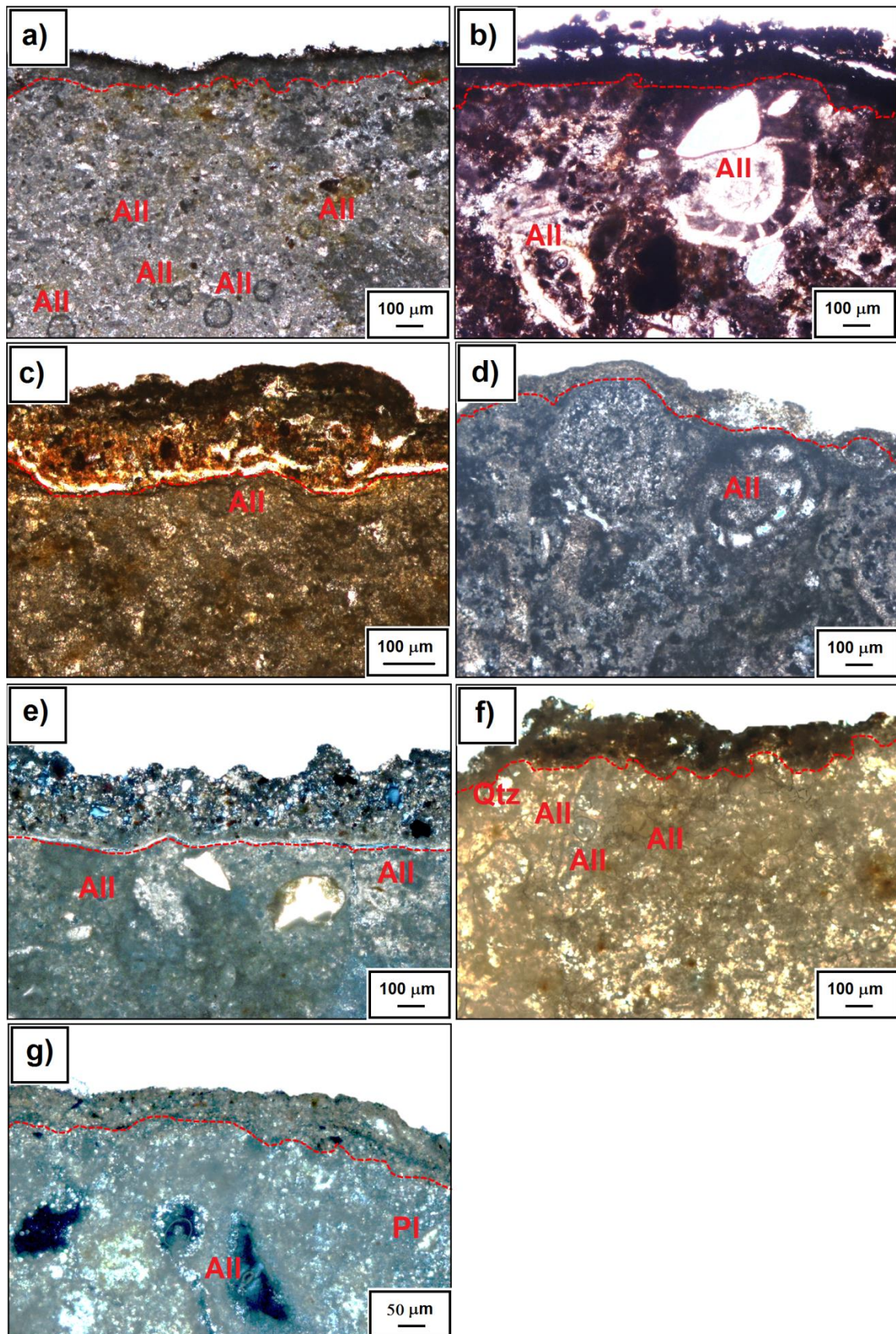


Fig. 2 Microphotographs in OM showing the main textural features of the limestones and the superficial layer associated. The red lines highlight the contact between the two components. The allochems present are indicated respectively with "All" (fossils and bioclasts), "Pl" (plagioclase), "Qtz" (quartz). A sample and relative image were selected for each study site. a) Sample 4, site 1 (Crossed Polarized Light view - CPL). b) Sample 5, site 2 (Plane Polarized Light view - PPL). c) Sample 10, site 3 (CPL). d) Sample 18, site 4 (CPL). e) Sample D, site 5 (PPL). f) Sample G, site 6 (CPL). g) Sample I, site 7 (CPL)

Ion chromatography

Several ionic species can be detected in building stones (Arnold 1983; Goudie and Viles 1995), in particular sulphates, chlorides and nitrates. In Fig. 3a, it has been reported the concentrations expressed in ppm of several cations and anions measured in black crusts samples. It is clear that calcium and sulphate ions are the most abundant species because the black crust is mainly made of gypsum, which has a solubility of about 2.5 g/l, and the preparation procedure of the sample for IC analysis leads to the complete dissolution of the gypsum. This statement is corroborated by the ionic trend of calcium and sulphate ions shown in Fig. 4. Those trends, which report the ppm concentrations in each sample, show a superimposition of the curves revealing a strong correlation between calcium and sulphate. In Fig. 3b, it has been reported the concentrations of analysed ions, excluding calcium and sulphate. It shows that sodium and chloride ions have the highest concentrations, suggesting the presence of sodium chloride, especially in samples 17, 10 and 9.

Sulphates are common degradation products coming from different sources and present mostly on masonries of both ancient and modern buildings, but, also on frescoes and wall paintings. They crystallize in three different forms such as gypsum ($\text{CaSO}_4 \cdot 2\text{H}_2\text{O}$), mirabilite ($\text{Na}_2\text{SO}_4 \cdot 10\text{H}_2\text{O}$) and epsomite ($\text{MgSO}_4 \cdot 7\text{H}_2\text{O}$) (Arnold 1983; Borrelli 1999).

Atmospheric pollution provides the most relevant contribution to their crystallization processes thanks to the high concentration of sulphur dioxide available. In fact, it combined with the air-humidity, reacts with the calcium carbonate present in the masonry constituents (i.e. mortars, stones, concrete, etc.) and produces calcium sulphates (Borrelli 1999). Additionally, some cements as Portland originally contain already low percentages of calcium sulphate (~ 4%).

Otherwise, the salts can be deposited directly from particulate matter on the surfaces.

Moreover, sulphates can precipitate from water rising for capillary action from the subsoil. They can derive from ammonium sulphate used in agriculture.

Lastly, sulphates-sources can be considered also, sea-spray and the biological activity of some micro-organisms. These are able to metabolize compounds in calcareous materials, containing reduced forms of sulphur and oxidize them to sulphates (Caneva et al. 1991)

Chlorides based salts are the most common ones and can be produced from various sources such as sea aerosol, groundwater loaded with salts, impurities in mortars, concretes, natural stones and other building materials, emissions into the atmosphere of hydrochloric acid coming from different industrial activities. Some stones naturally contain chlorides, as it is the case for Egyptian limestone (Gauri 1981; Aly et al. 2015). The high solubility makes the Chlorides highly damaging because they can migrate deeply and crystallize into stone materials producing intense sub efflorescence and consequently micro-cracks and the destruction of the pore structure (Borrelli 1999; Fitzner et al. 2002).

In particular, Halite (NaCl) is the predominant salt species in Egyptian soil and one of the most damaging (Fitzner et al. 2002; Khallaf 2011; Abdelmegeed and Hassan 2019). Its abundance in Historic Cairo buildings was due to the combination of surrounding deterioration factors, especially groundwater, sewage, and lack of infrastructure system (Abdelmegeed and Hassan 2019).

Nitrates were also found in all samples, with peaks in 6, 17, 18 and I. Their production is closely relative to the nitrogen pollutants present in the atmosphere and linked for example to the domestic and industrial fuel burnings (Khallaf 2011) or to the photochemical smog, commonly diffused in areas with high rates of pollution combined with long periods of solar radiation.

The organic decomposition of the nitrogen-products present in the soil or in the walls can induce the production of Nitrites. Their main source is attributable to the infiltration of sewage and this can be the case as most of the foundations and walls of the Islamic monuments in historic Cairo have been affected by the flooding of the sewage water (El-Metwally and Ramadan 2004). Nitrates may exist also in ground soil as a result of decaying organic material. In this regard, Fitzner et

al. (2002) underline how the water table (groundwater, subsoil water) has significantly risen during the last decades in Historic Cairo and in extreme cases has reached the ground floor of monuments. This situation accentuated the insufficiency or even the absence of sewage systems, causing an increase in water pollution. Nevertheless, the tendency for nitrites (NO_2^-) to oxidize to nitrates (NO_3^-) makes it difficult to find them in masonry (Borrelli 1999).

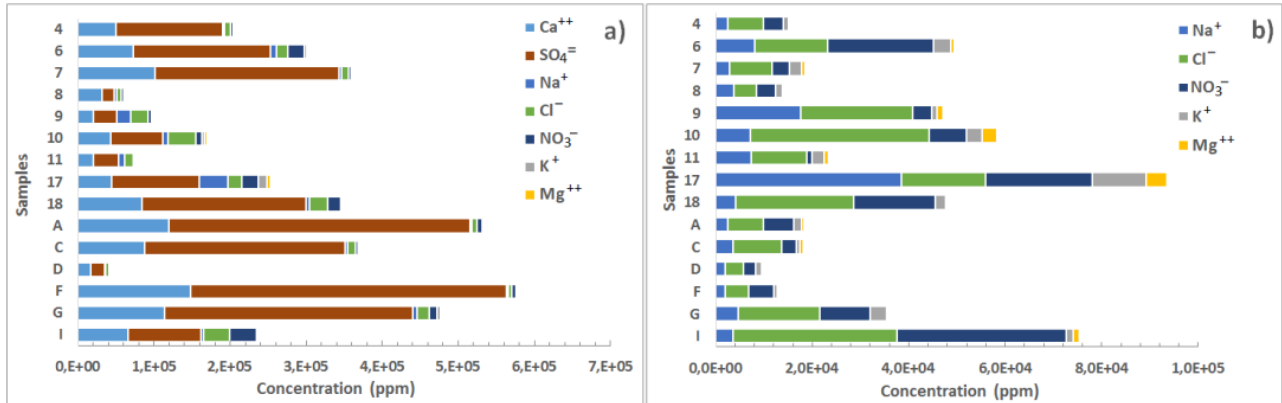


Fig. 3 Ionic concentrations measured in samples: chart a) contains all considered ions, while in chart b) calcium and sulphate ions are excluded

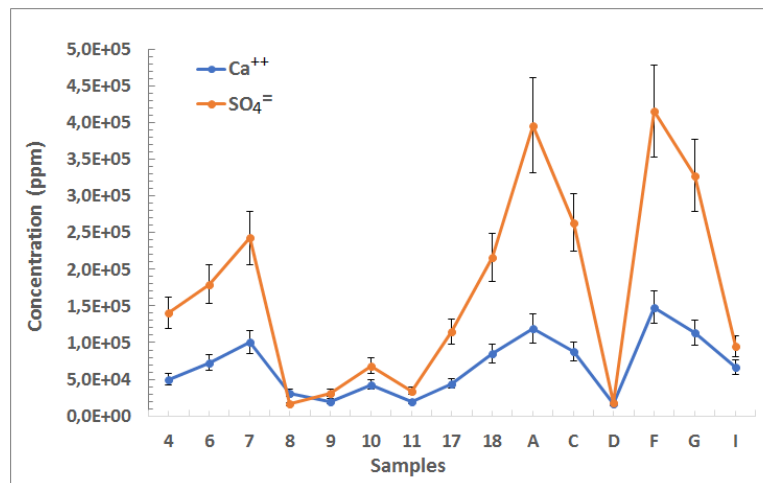


Fig. 4 Concentrations trends in samples of sulphate and calcium ions

FT-IR analysis

Table 3 displays FT-IR data obtained on the analysed samples and Fig. 5 shows some representative spectra. The main components detected in all the crusts are gypsum, oxalate and calcite, typical black crusts compounds. Precisely, spectra show the characteristic absorption peaks of gypsum centred at 672, 1109, 1684, 3397 and 3533 cm^{-1} , as well as the stretching and bending vibrations of the calcium carbonate, with peaks at 1405, 872 and 712 cm^{-1} can be certainly ascribable to the underlying substrate (Vahur et al. 2016).

Table 3 reports the qualitative estimates expressed in percentages based on the intensity of the peaks. In this regard, gypsum is the most abundant mineralogical species; its relative abundance varies from >50 (samples 4, 10, 17, 18, A, D, F, G e I) to 20-50% (samples 5, 7, 8, e C). Also, calcite varies from 10-5% (samples 7, 8, 9, 10, 18, D e I) to 1-5% (4, 6, 17, A, C, F e G) according to the qualitative valuation. Finally, oxalates (with peaks at 1618, 1321 and 780 cm^{-1}) and silicates (peaks centred between 1000–1030 cm^{-1}) are rather scarce not exceeding 5%.

The presence of oxalate, according to the scientific literature, could be related to restoration works carried out in the past or to the presence of biological activity (Griffin et al. 1991; El-Metwally and Ramadan 2004; Barone et al. 2008; Belfiore et al. 2010, 2013; Gulotta et al. 2013).

The origin of silicates, instead, could be ascribable to two sources: primary, namely from the substrate where they are naturally present; or secondary, from the deposit of soil dust. In the first case, in fact, during the sulphation process minerals such as quartz, present in the substrate, do not undergo the attack of sulfuric acid and can be incorporated into the crust during the gypsum precipitation process.

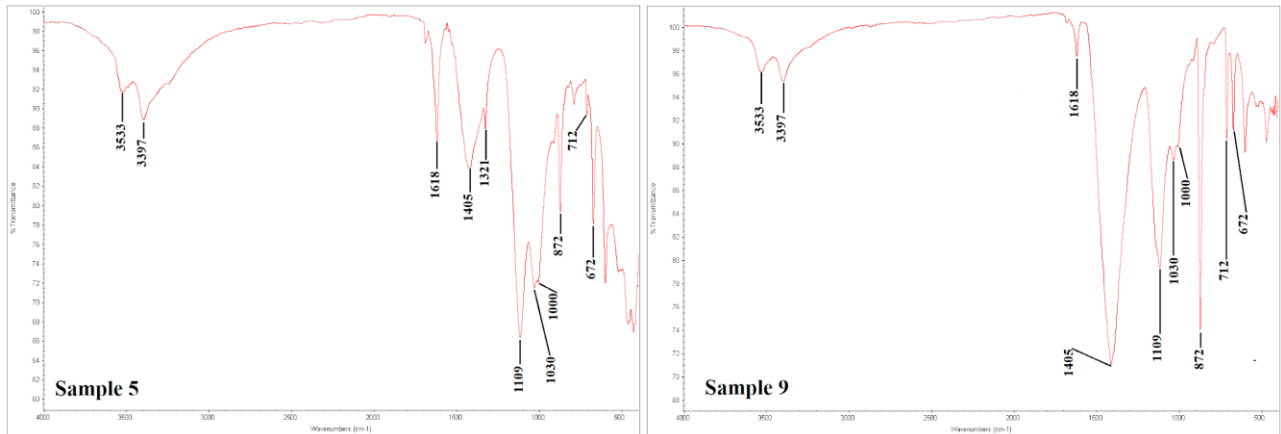


Fig. 5 FT-IR spectra of representative crust of samples 5 and 9

Table 3 Mineralogical composition of the crusts collected in Cairo monuments by FT-IR (Gypsum; Calcite; Oxalates, and Silicate). Legend: + + + + +: > 50%; + + + +: 20-50%; + + +: 10-20%; + +: 10-5%; +: 1-5%

	Samples ID	Gypsum	Calcite	Oxalates	Silicates
Site 1	4	+++++	+	+	+
	6	++++	+	+	+
Site 2	5	++++	+	+	+
	7	++++	++	+	+
Site 3	8	++++	++	+	+
	9	++++	++	+	+
	10	+++++	++	+	+
Site 4	17	+++++	+	+	+
	18	+++++	++	+	+
Site 5	A	+++++	+	+	+
	C	++++	+	+	+
	D	+++++	++	+	+
Site 6	F	+++++	+	+	+
	G	+++++	+	+	+
Site 7	I	+++++	++	+	+

Carbonaceous fraction

The carbonaceous material (total carbon, TC) is classified into elemental carbon (EC) (better known as black carbon (BC)), and organic carbon (OC). The analysis of these components is of great interest for the study of black crusts (La

Russa et al. 2017). The EC fraction has a graphitic structure and represents a primary pollutant, directly emitted during the combustion processes. The OC fraction is composed of different classes of compounds (e.g. hydrocarbons, oxygenated) and may have a primary or secondary origin. The carbonaceous components are involved in some heterogeneous chemical reactions that occur in the atmosphere, acting with SO₂, NO₂, O₃ and other gaseous components (Avino et al. 2000, 2002; Atkinson et al. 2003; Donahue et al. 2005); they are also responsible for some degradation processes, accelerating the corrosion phenomena of metals or the formation of black crusts (Barca et al. 2014; Comite et al. 2012, 2017, 2019, 2020; La Russa et al. 2013, 2017, 2018; Ruffolo et al. 2015). In addition to EC and OC, the carbonaceous fraction (TC) of the black crusts also includes the CC (carbonatic carbon), coming from the stone substrate and oxalates (Ox), whose origin may depend on different factors as previously described in the FT-IR/ATR study.

Table 4 shows the carbon fraction detected in the analysed samples and the various ratios of OC/EC, EC/TC, and OC/TC.

Table 4 TC (total carbon); OC (organic carbon); EC (elemental carbon); OX (oxalate), CC (carbonate carbon), Gy (gypsum) concentrations (wt.%) achieved in the degradation layers analysed.

Site	Sample ID	Height of sampling	OC	EC	OX	CC	TC	Gy
Site 1	4	2,50 m	1.33	1.50	0.11	3.66	6.60	22.97
	6	35 cm	1.20	2.73	0.13	3.12	7.18	26.44
Site 2	5	25 cm	1.19	2.89	0.34	3.03	7.45	6.01
	7	1,55 m	1.20	1.33	0.34	3.03	5.90	36.00
Site 3	8	45 cm	1.58	5.44	0.33	6.01	13.36	1.53
	9	20 cm	1.88	5.95	0.14	7.22	15.19	1.32
	10	30 cm	1.85	1.95	0.11	7.23	11.14	7.01
Site 4	17	20 cm	0.56	2.85	0.26	5.11	8.78	15.57
	18	2 m	0.86	1.15	0.12	3.15	5.28	30.99
SITE 5	A	90 cm	1.11	1.56	0.23	5.22	8.12	50.46
	C	2 m	0.36	0.99	0.22	3.99	5.56	36.57
	D	50 cm	1.15	2.65	0.12	2.45	6.37	1.50
Site 6	F	1 m	0.99	1.88	0.12	5.11	8.10	55.60
	G	50 cm	0.78	2.69	0.10	4.99	8.56	49.48
Site 7	I	90 cm	0.99	2.45	0.18	6.78	10.40	12.45

The samples show a variable content in TC (Table 4) ranging from a maximum of about 15 (for sample 9) to a minimum of about 5 (for sample 18).

Different OX (oxalate) and CC (carbonatic carbon) values were observed for the different crust samples analysed, as, coherently, already recognized in the IR analysis (La Russa et al. 2017, 2018) (Table 3).

High CC values were detected for most of the samples (i.e. 8, 9, 10, 17, F and I), suggesting a possible greater susceptibility to substrate degradation over time (Comite et al. 2018; La Russa et al. 2017, 2018). Overall, the data show that all the samples have higher EC contents than OC. Specifically: a) the highest EC values (wt.%) were detected in samples 8, 9 (approximately 6); b) intermediate values in samples 5, 6, 17, D and G (approximately 3) and c) the slightly lower values in samples 4, 7, 18, A, C, F and I (between about 2.5 and 1).

As is well known, the EC (or black carbon) represents the factor that determines the colouring of the black crust (Ghedini et al. 2006; Tidblad et al. 2012; Fermo et al. 2015); therefore a great amount within the degradation layer can affect greater damage on the monument's surface. Indeed, the dark colouring produces a different susceptibility to absorb solar radiation, causing a greater dilation of the altered stone material compared to the unaltered one. Besides, the difference

linear expansion, due to the linear expansion coefficient of calcium sulphate (i.e. the main component of the crust) which is greater than that revealed in the carbonatic stone substrate, could lead to greater damage in the calcareous materials characterizing the studied monuments.

Fig. 6 shows the values of OC (wt.%) and EC (wt.%) obtained in relation to the site and the sampling height. The histograms suggest how the values of the OC and EC components decrease as the sampling height increases, highlighting a good correlation between them.

Data indicate that the lower surfaces of the studied monuments are more affected by the deposition processes compared to the higher ones; consequently, they may be affected by greater exposure to the damage processes induced by pollution. A larger amount of the two carbon components OC and EC was observed in the samples 9 and 10 taken at about 20-30 cm from the walking surface; lower accumulations were instead observed mainly in samples taken between 200-250 cm in height. Moreover, it is also evident that there is no correlation between the values obtained at the same height in different sites.

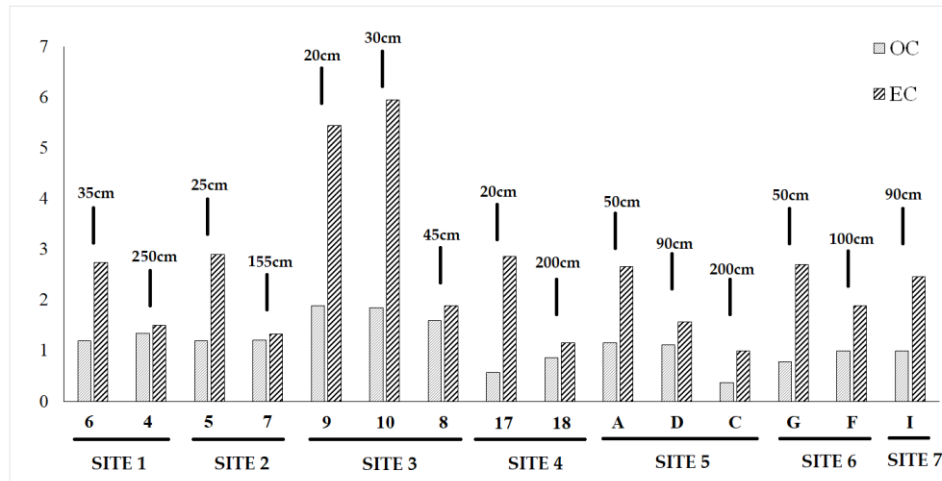


Fig. 6 OC and EC values (wt.%) obtained in the different specimens in relation to the sampling height

Generally, the formation of black crusts is conditioned by various factors, firstly the deposition surfaces, washouts and exposure to polluting sources. The identification of these latter ones, by the means of OC and EC concentrations, is crucial in the study area. In fact, they should provide precious information about the main degradation processes affecting the surfaces examined.

The scatter plots show the OC and EC (fig. 7a, b) concentrations for each sample taken at the low heights (sample 5, 6, 9, 10 and 17, heights ranging from 20 to 35 cm) (Fig. 7a) and high heights (sample 4, 7, 18, A, C, F and I, heights ranging from 90 to 250 cm) (Fig.7b). Strong correlations between OC and EC have been found for samples coming from low heights ($R^2 = 0.7917$). This data indicates that the carbonaceous fraction detected on these surfaces originated mainly from common sources and also influenced by similar transport processes (Na et al. 2020). Conversely, the samples taken at higher heights (i.e. samples 4, 7, 18, A, C, F and I, height between 90 and 250 cm), showed relatively poor correlations ($R^2 = 0.1385$) which could indicate that the carbonaceous fraction on the surfaces has different origins (Na et al. 2020).

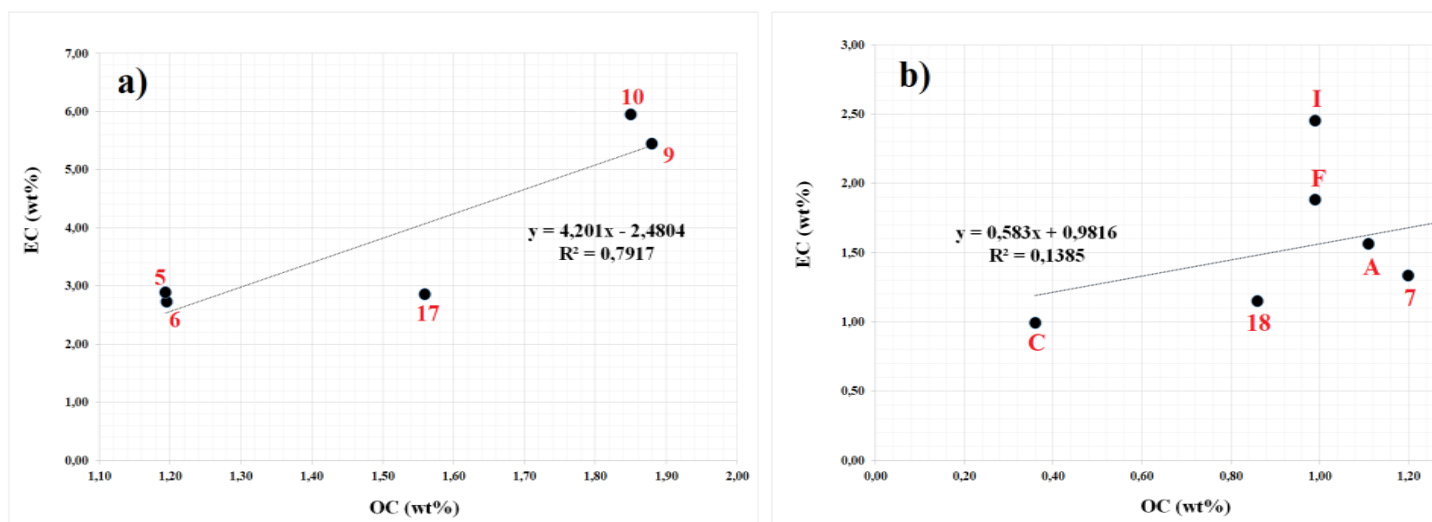


Fig. 7 Scatter plots of OC and EC concentrations for the samples a) sample 5,6,9,10, 17 taken at low heights; b) sample 4, 7, 18, A, C, F and I taken at high heights.

State of conservation and proposals of intervention strategies

The substrates analysed show within a fair state of conservation, even if the incipient fractures and the observed dissolution phenomena represent probable predisposing factors for the development of further degradation processes. The study conducted affirms that currently, the most harmful decay phenomena affect the superficial portions of the stone substrates. Indeed, it was identified mainly black crusts rich in gypsum, soluble salts (e.g. nitrates, chlorides), as well as accumulation of other pollutants how the determination of carbonaceous fraction suggested. The analyses carried out highlighted how environmental pollution, primarily air pollution, constitutes the main threat to the conservation of monuments in Historic Cairo. Moreover, the data collected underline the need for targeted interventions based on a detailed characterization of the degradation products. In fact, the choice of the most suitable methods can depend, for

example, from the morphology and extension of black crusts above and inside the substrate and, in the case of soluble salts, from their different behaviour.

There are, in fact, two types of salts: slightly soluble and highly soluble salts. Gypsum is the main exponent of the slightly soluble salts (Arnold 1983). They produce more intense damages because they crystallize immediately below the surface causing bulging, detachment and loss of fragments.

Highly soluble salts include chlorides and nitrates (Arnold 1991). They can produce dark patches on the substrate thanks to their capacity to reach very high concentrations of highly hygroscopic salts that remain in solution in humid environments.

Conversely, they produce efflorescence phenomena in dry conditions.

Generally, the damages caused by the highly soluble salts are limited to a superficial decohesion, being necessary too high rates of evaporation for triggering a really harmful salt crystallization.

Overall, the variability and the complexity of the decay phenomena make it necessary to plan specific interventions, capable of mitigating the action of degradation processes such as the above-mentioned formation of black crusts and crystallization of soluble salts.

In this regard, it would be preferred to adopt suitable cleaning techniques such as laser cleaning in the case of black crusts or periodic treatments based on cellulose pulp packs or using special clays like sepiolite for the extraction of soluble salts from the substrates.

Moreover, it could be useful to plan the application of protective and consolidant treatments selected on the basis of the nature of the substrate and the type of degradation product, in order to extend the effects of cleaning procedures and preserve a good state of conservation of the built heritage over time.

Conclusion

Historic Cairo represents one of the most representative examples of Islamic architecture. Unfortunately, the built cultural heritage is affected by different and harmful degradation phenomena closely linked, firstly, to the intense environmental pollution and secondly to the intrinsic features of the stone materials used. Seven monumental sites were selected on the basis of their conservation state and eighteen samples of the stone substrate with relative degradation products, mainly black crusts, were taken and analysed by complementary analytical techniques.

Results indicated that the black crusts are generally well adherent to the limestone substrates and present variable thickness, with no particular correlation with the site of provenance. The analyses suggested how the crusts are mainly composed of gypsum with lower content of calcite and oxalates. These latter ones could be related to past restoration works or to the decay produced by biological activity. The IC analyses underlined the great contribution of salts as degradation agents, namely chlorides, nitrates, and nitrites. They are produced mainly by anthropic activities such as industry and vehicular traffic and secondly by natural sources as sea spray.

In addition, the determination of the carbonaceous fraction suggests the high incidence of the pollution in the degradation processes affecting the substrates analysed. Besides, according to the measurements of the organic and elemental carbon of the degraded layers, the lower surfaces of the studied monuments are more affected by the deposition process compared to the higher ones.

Overall, the methodological approach applied in this study, allowed to collect crucial data about environmental pollution in Historic Cairo to implement with further sampling campaigns in the next researches. It will allow to trace a base-

mapping of the conservation state of the built heritage, in the area, defining both the main polluting sources and the development of the relative degradation products to investigate more deeply in future studies.

This will provide essential information to conceive effective conservation strategies and suitable restoration interventions based on appropriate cleaning procedures, consolidating and protective products capable of preserving the built Cultural Heritage of Historic Cairo over time.

Acknowledgments

The research is part of the Executive program for scientific cooperation between the Italian Republic and the Arab Republic of Egypt, entitled “Characterization of black crusts formed on historical buildings under different levels of ambient air pollution in Cairo and Venice”.

Reference

- Abdelmegeed M, Hassan S (2019) Diagnostic investigation of decaying limestone in historical buildings at the Mamluks Cemetery- City of the Dead, Egypt. *EJARS* 9(2): 183-196. DOI: 10.21608/ejars.2019.66989.
- Aly N, Hamed A, Abd El- Al A. (2020) The Impact of Hydric Swelling on the Mechanical Behavior of Egyptian Helwan Limestone. *Periodica Polytechnica Civil Engineering*. <https://doi.org/10.3311/PPci.15360>.
- Aly N, Wangler T. Török Á (2018) The effect of stylolites on the deterioration of limestone: possible mechanisms of damage evolution. *Enviro Earth Sci* 77:565.
- Aly N, Gomez-Heras M, Hamed A, Álvarez de Buergo M, Solimane F (2015) The influence of temperature in a capillary imbibition salt weathering simulation test on Mokkattam limestone *Materiales de Construcción. Mater. Construc* 65:317. <http://dx.doi.org/10.3989/mc.2015.00514>.
- Anoniou J (1999) *Historic Cairo. A Walk through the Islamic City* by Jim Anoniou Publisher. The American University in Cairo Press.
- Araoz G (2008) Annual report, International Council On Monuments and Sites (ICOMOS), Paris.
- Arnold B (1983) Determination of mineral salts from monuments. *Stud Conserv* 29:129-138. <https://doi.org/10.1179/sic.1984.29.3.129>.
- Arnold A, Zehnder K (1991) Monitoring wall paintings affected by soluble salts. In: Cather S (ed) *The Conservation of wall paintings*. Getty Conservation Institute, Marina del Rey (California), pp 103-135.
- Atkinson R, Arey J. (2003) Gas-phase tropospheric chemistry of biogenic volatile organic compounds: A review. *Atmos Environ*, 37:197-219. doi: 10.1016/S1352-2310(03)00391-1.
- Avino P, Brocco D, Cecinato A, Lepore L, Balducci C. (2002) Carbonaceous components in atmospheric aerosol: Measurement procedures and characterization. *Ann Chim* 92:333-341.
- Avino P, Brocco D, Lepore L, Ventrone I. (2000) Fundamental aspects of carbonaceous particulate measurements in the study of air pollution in urban area. In: J.W.S. Longhurst et al. (eds) *Air Pollution VIII*, Cambridge University, UK, pp. 301-309.
- Barca D, Comite V, Belfiore CM, Bonazza A, La Russa MF, Ruffolo SA, Crisci G, Pezzino A, Sabbioni C (2014) Impact of air pollution in deterioration of carbonate building materials in Italian urban environments. *Appl Geochem*, 48:122-131. DOI: 10.1016/j.apgeochem.2014.07.002.
- Barone G, La Russa MF, Lo Giudice A, Mazzoleni P, Pezzino A (2008) The Cathedral of S. Giorgio in Ragusa Ibla (Italy): characterization of construction materials and their chromatic alteration. *Environ Geol* 55:499-504.

- Belfiore CM, Barca D, Bonazza A, Comite V, La Russa MF, Pezzino A, Sabbioni C. (2013) Application of spectrometric analysis to the identification of pollution sources causing cultural heritage damage. *Environ Sci Pollut Res* 20:8848-8859. DOI:10.1007/s11356-013-1810-y.
- Belfiore CM, La Russa MF, Pezzino A, Campani E, Casoli, A. (2010) The baroque monuments of Modica (Eastern Sicily): assessment of causes of chromatic alteration of stone building materials. *Appl Phys A Mater Sci Process* 100:835-844.
- Borrelli E (1999) Conservation of architectural heritage, historic structures and materials. *Salts*. ICCROM, Rome, Italy.
- Cachier H, Bremond MP, Buat-Menard P (1989) Determination of atmospheric soot carbon with a sample thermal method. *Tellus Ser B Chem Phys Meteorol* 41:379-390. <https://doi.org/10.3402/tellusb.v41i3.15095>.
- Caneva G, Nugari MP, Salvadori O (1991) Biology in the Conservation of Works of Art. ICCROM, Rome, pp 88-91.
- Comite V, Pozo-Antonio JS, Cardell C, Rivas T, Randazzo L, La Russa MF, Fermo P Environmental impact assessment on the Monza Cathedral (Italy): a multi-analytical approach. *Int. J. Conserv. Sci.*, 2020, 11, Special Issue 1, 291-304.
- Comite V, Pozo-Antonio JS, Cardell C, Rivas T, Randazzo L, La Russa MF, Fermo P. Metals distributions within black crusts sampled on the facade of an historical monument: The case study of the Cathedral of Monza (Milan, Italy). In 2019 IMEKO TC4 International Conference on Metrology for Archaeology and Cultural Heritage, *MetroArchaeo*, 2019, 73-78
- Comite V, Fermo P (2018) The effects of air pollution on cultural heritage: the case study of Santa Maria delle Grazie al Naviglio Grande (Milan). *Eur Phys J Plus* 133: 556. <https://doi.org/10.1140/epjp/i2018-12365-6>.
- Comite V, Barca D, Belfiore CM, Bonazza A, Crisci GM, La Russa MF, Pezzino A, Sabbioni C (2012) Potentialities of spectrometric analysis for the evaluation of pollution impact in deteriorating stone heritage materials. In: Critelli S et al. (eds) *Rendiconti online della Società Geologica Italiana*. 86 Congresso Nazionale della Società Geologica Italiana, Arcavacata di Rende, 21:652-653.
- Davidson CI, Tang F, Finger S, Etyemezian V, Sherwood SI (2000) Soiling patterns on a tall limestone building: changes over 60 years. *Environ Sci Technol* 34:560-565.
- Delgado Rodrigues J, Ferreira Pinto AP (2019) Stone consolidation by biomineralisation. Contribution for a new conceptual and practical approach to consolidate soft decayed limestones. *J Cult Herit* 39:82-92.
- Donahue NM, Huff Hartz KE, Chuong B, Presto AA, Stanier CO, Rosenhørn T, Robinson AL, Pandis SN (2005) Critical factors determining the variation in SOA yields from terpene ozonolysis: A combined experimental and computational study. *Faraday Discuss* 130: 295-309. doi: 10.1039/b417369d.
- Dunham RJ (1962) Classification of carbonate rocks according to depositional textures. *Amer Assoc Petrol Geol Mem* 1:108-121.
- El-Metwally AA, Ramadan AB (2004) The Role of Air Pollutants and Sewage Waste in Acceleration of Degradation of the Islamic Cultural Heritage of Cairo. In: Linkov I, Ramadan AB (eds). *Comparative Risk Assessment and Environmental Decision Making*. *Nato Science Series: IV: Earth and Environmental Sciences*, 38, Springer, Dordrecht.
- Fermo P, Turrión GR, Rosa M, Omegna A (2015) A new approach to assess the chemical composition of powder deposits damaging the stone surfaces of historical monuments. *Environ Sci Pollut Res* 22:6262-6270. DOI 10.1007/s11356-014-3855-y
- Fitzner B, Heinrichs K, La Bouchardiere D (2002) Weathering damage on Pharaonic sandstone monuments in Luxor-Egypt. *Build Environ* 38:1089-1103. DOI: 10.1016/S0360-1323(03)00086-6.

- Fitzner B, Heinrichs K, La Bouchardiere D (2000) Damage index for stone monuments. In: Galan E, Zezza F (Eds.) *Protection and Conservation of the Cultural Heritage of the Mediterranean Cities*. In: *Proceedings of the 5th International Symposium on the Conservation of Monuments in the Mediterranean Basin*, Sevilla Spain, 315-326.
- Folk RL (1959) Practical petrographic classification of limestones. *Bull Amer Assoc Petrol Geol* 43:1-38.
- Gauri KL (1981) The Deterioration of Ancient Stone Structures in Egypt. In *Prospection et Sauvegarde des Antiquités de l’Egypte: Actes de la Table Ronde organisée à l’occasion du Centenaire de l’Institut Français d’Archéologie Orientale*. Grimal NC (ed). *Bibliothèque d’Etude*, Le Caire: Institute Francais d’Archeologie Orientale du Caire.
- Ghedini N, Sabbioni C, Bonazza A, Gobbi G (2006) Chemical-thermal quantitative methodology for carbon speciation in damage layers on building surfaces. *Environ Sci Technol* 40:939-944.
- Gomez-Heras M, Fort R (2007) Patterns of halite (NaCl) crystallisation in building stone conditioned by laboratory heating regimes. *Environ Geol* 52:259-267.
- Goudie AS, Viles HA (1995) The nature and pattern of debris liberation by salt weathering: a laboratory study. *Earth Surf Proc Land* 20:437-449. <https://doi.org/10.1002/esp.3290200505>.
- Griffin PS, Indictor N, Koestler RJ (1991) The Biodeterioration of Stone: a Review of Deterioration Mechanisms, Conservation Case Histories, and Treatment. *Internat Biodet* 28:187-207.
- Gulotta D, Bertoldi M, Bortolotto S, Fermo P, Piazzalunga A, Toniolo L (2013) The Angera stone: a challenging conservation issue in the polluted environment of Milan (Italy). *Environ. Earth Sci.* 69:1085-1094.
- Kanakidou M, Seinfeld JH, Pandis SN, Barnes I, Dentener FJ, Facchini MC, Van Dingenen R, Ervens B, Nenes A, Nielsen CJ, Swietlicki E, Putaud JP, Balkanski Y, Fuzzi S, Horth J, Moortgat GK, Winterhalter R, Myhre CEL, Tsigaridis K, Vignati E, Stephanou EG, Wilson J (2005) Organic aerosol and global climate modelling: A review. *Atmos Chem Phys* 5:1053-1123. <https://doi.org/10.5194/acp-5-1053-2005>.
- Kavouras IG, Stephanou EG (2002) Direct evidence of atmospheric secondary organic aerosol formation in forest atmosphere through heteromolecular nucleation. *Environ Sci Technol* 36:5083-5091. doi: 10.1021/es025811.
- Khallaf MK (2011) Effect of Air Pollution on Archaeological Buildings in Cairo. In: Chmielewski A (ed) *Monitoring, Control and Effects of Air Pollution*. IntechOpen, London, pp 179-200.
- Klemm DD, Klemm R (2001) The building stones of ancient Egypt - a gift of its geology. *J Afr Earth Sci* 33:63-642.
- La Russa MF, Comite V, Aly N, Barca D, Fermo P, Rovella N, Antonelli F, Tesser E, Aquino M, Ruffolo SA (2018) Black crusts on Venetian built heritage, investigation on the impact of pollution sources on their composition. *Eur Phys J Plus* 133:370. DOI: 10.1140/epjp/i2018-12230-8.
- La Russa MF, Fermo P, Comite V, Belfiore CM, Barca D, Cerioni A, De Santis M, Barbagallo LF, Ricca M, Ruffolo SA (2017) The Oceanus statue of the Fontana di Trevi (Rome): the analysis of black crust as a tool to investigate the urban air pollution and its impact on the stone degradation. *Sci Total Environ.* 593-594:297-309.
- La Russa MF, Belfiore CM, Comite V, Barca D, Bonazza A, Ruffolo SA, Pezzino A. (2013) Geochemical study of black crusts as a diagnostic tool in cultural heritage. *Appl Phys A-Mater* 113: 1151-1162. DOI:10.1007/s00339-013-7912-z.
- Na L, Xin W, Weizheng H, Siyue S, Jinghui Wu (2020) Characteristics and temporal variations of organic and elemental carbon aerosols in PM1 in Changchun, Northeast China. *Environ Sci Poll Res* 27:8653-8661.
- Monte MD (1991) Stone monument decay and air pollution. In: Corso I (ed) *Weathering and air pollution*, *Comunità delle Università Mediterranee, Scuola Universitaria C.U.M. Conservazione dei Monumenti*, 101-10.

- Pires V, Silva ZSG, Simã JAR, Galhano C, Amaral PM (2010) “Bianco di Asiago” limestone pavement. Degradation and alteration study. *Constr build mater* 24:6866-94. <https://doi.org/10.1016/j.conbuildmat.2009.10.040>.
- Ruffolo SA, Comite V, La Russa MF, Belfiore CM, Barca D, Bonazza A, Crisci GM, Pezzino A, Sabbioni C (2015) Analysis of black crusts from the Seville Cathedral: A challenge to deepen understanding the relationship among microstructure, microchemical features and pollution sources. *Sci Tot Environ* 502:157-166.
- Schaap M, Denier Van Der Gon, HAC, Dentener, FJ, Visschedijk, AJH, Van Loon, M, ten Brink, HM, Putaud, J-P, Guillaume B, Lioussé C, Builtjes, PJH (2004) Anthropogenic black carbon and fine aerosol distribution over Europe. *J Geophys Res Atmos* 109:11-16. doi: 10.1029/2003JD004330.
- Tidblad J, Kucera V, Ferm M et al (2012) Effects of air pollution on materials and cultural heritage: ICP materials celebrates 25 years of research. *Int J Corros* 2012:1-16.
- Turpin BJ, Huntzicker JJ (1995) Identification of secondary organic aerosol episodes and quantitation of primary and secondary organic aerosol concentrations during SCAQS. *Atmos Environ* 29:3527-3544. doi: 10.1016/1352-2310(94)00276-Q.
- Vahur S, Teearu A, Peets P, Joosu L, Leito I. (2016) ATR-FT-IR spectral collection of conservation materials in the extended region of 4000-80 cm⁻¹. *Anal Bioanal Chem* 408:3373-3379. <https://doi.org/10.1007/s00216-016-9411-5>.
- Yttri KE, Aas W, Bjerke A, Cape JN, Cavalli F, Ceburnis D, Dye C, Emblico L, Facchini MC, Forster C, Hanssen JE, Hansson HC, Jennings SG, Maenhaut W, Putaud JP, Torseth K (2007) Elemental and organic carbon in PM₁₀: A one year measurement campaign within the European Monitoring and Evaluation Programme EMEP. *Atmos Chem Phys* 7:5711-5725. <https://doi.org/10.5194/acp-7-5711-2007>.
- Watchman A (1990) A summary of occurrences of oxalate-rich crusts in Australia. *Rock Art Res* 7:44-50.
- Williams C (2004) *Islamic Monuments in Cairo: The Practical Guide*. American University in Cairo Press.